Sterically Demanding Diporphyrin Ligands and Rhodium(II) Porphyrin Bimetalloradical Complexes

Xiao-Xiang Zhang and Bradford B. Wayland*

Department of Chemistry, University of Pennsylvania, Philadelphia, Pennsylvania 19104-6323

Received June 12, 2000

A series of sterically demanding diporphyrins H_2(por)−X−(por)H_2 ligands that contain spacers (X) with different degrees of flexibility were synthesized from the trimesitylporphyrin derivatives 5-(4-hydroxyphenyl)-10,15,20-trimesitylporphyrin (TMP-OH)H_2 (1a) and 5-(2,6-dimethyl-4-hydroxyphenyl)-10,15,20-trimesityl-porphyrin, (DMTMP-OH)H_2 (**1b**). The monomeric porphyrins **1a,b**, which have steric demands similar to that of tetramesitylporphyrin, (TMP)H_2, and carry a hydroxyl functional group at the *para* position of one of the *meso*-phenyl substituents, were constructed from reaction of pyrrole with two aromatic aldehydes by a mixed aldehyde condensation approach. The diporphyrins with alkyl diether tethers were obtained stepwise from reactions of the hydroxy functionalized porphyrins **1a,b** with dibromides $Br(CH_2)_nBr$. The diporphyrin which contains a more rigid *m*-xylylene spacer, was made directly from reaction of **1b** with α,α′-dibromo-*m*-xylene. Rhodium was inserted into the porphyrins using $Rh_2(CO)_2Cl_2$ and converted to dimethyl complexes Me−Rh(Por)−X−(Por)Rh−Me. The dirhodium(II) derivatives ·Rh(por)−X−(por)Rh·) were generated by photolysis of the dimethyl complexes and observed to occur as stable bimetalloradicals because the ligand steric demands prohibit Rh(II)−Rh(II) bonding. EPR spectra of the dirhodium(II) derivatives, triphenyl phospine adducts, and dioxygen complexes are reported. The kinetic advantage of bimetalloradical complexes for substrate reactions that have two metal-centered radicals in the transition state is demonstrated by reactions of dihydrogen with dirhodium(II) bimetalloradical complexes.

Introduction

Metalloradical (M·) reactions with substrates such as H_2 and CH_4, where atom abstractions are highly endothermic, can proceed by a concerted interaction of two metalloradicals with the substrate through a four-centered transition state.[1−8] Reactions that utilize this type of pathway have relatively low

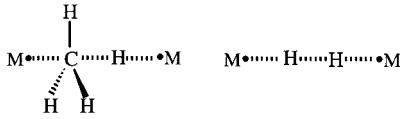

activation enthalpies because of extensive bond making in the transition state but generally occur slowly because of the large activation entropies associated with termolecular processes.[1−5] Reactions of (tetramesitylporphyrinato)rhodium(II) ((TMP)Rh^{II}·) with CH_4 and H_2 are examples of processes that occur by this termolecular pathway.[1−3] One potentially important consequence of this metalloradical mechanism is that there is a kinetic preference for methane activation over C−H bond reactions with all other aliphatic or aromatic hydrocarbons which is a different selectivity order from all other systems that activate hydrocarbons.[9−13] This selectivity has its origin in the steric demands of the termolecular transition state that favor the smaller substrate.[1,2,5]

A strategy to improve the kinetics and retain the selectivity of metalloradical reactions with substrates is to incorporate two metal centered radical sites into a single molecular unit which has the potential to convert the termolecular reaction into a bimolecular process.[7,8] This article reports on the design and

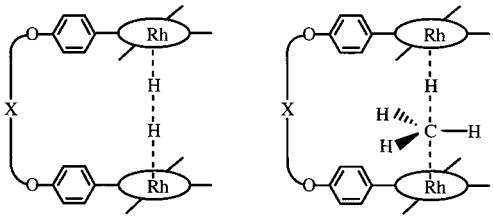

procedures for the synthesis of a series of diporphyrin ligands

(1) Sherry, A. E.; Wayland, B. B. *J. Am. Chem. Soc*. **1990**, *112*, 1259.
(2) Wayland, B. B.; Ba, S.; Sherry, A. E. *J. Am. Chem. Soc*. **1991**, *113*, 5305.
(3) Wayland, B. B.; Ba, S.; Sherry, A. E. *Inorg. Chem*. **1992**, *31*, 148.
(4) Simandi, L. I.; Budo-Zahonyi, E.; Szeverenyi, Z.; Nemeth, S. *J. Chem. Soc., Dalton Trans.* **1980**, 276.
(5) Halpern, J.; Pribinic, M. *Inorg. Chem*. **1970**, *9*, 2626.
(6) (a) Halpern, J. *Inorg. Chim. Acta* **1982**, *62*, 31. (b) Halpern, J. *Inorg. Chim. Acta* **1983**, *77*, L105.
(7) Zhang, X.-X.; Wayland, B. B. *J. Am. Chem. Soc*. **1994**, *116*, 7897.
(8) Zhang, X.-X.; Parks, G. F.; Wayland, B. B. *J. Am. Chem. Soc*. **1997**, *119*, 7938.
(9) (a) Hoyano, J. K.; McMaster, A.; Graham, W. A. G. *J. Am. Chem. Soc*. **1983**, *105*, 7190. (b) Rest, A. J.; Whitewell, I.; Graham, W. A. G.; Hoyano, J. K.; McMaster, A. D. *J. Chem. Soc., Chem Commun*. **1984**, 624. (c) Ghosh, C. K.; Graham, W. A. G. *J. Am.Chem. Soc*. **1983**, *109*, 4726. (d) Janowicz, A. H.; Bergman, R. G. *J. Am. Chem. Soc*. **1983**, *105*, 3929. (e) Wenzel, T. T.; Bergman, R. G. *J. Am. Chem. Soc*. **1986**, *108*, 4856. (f) Hackett, M.; Whitesides, G. M. *J. Am. Chem. Soc*. **1988**, *110*, 1449. (g) Harper, T. G.; Shinomoto, R. S.; Deming, M. A.; Flood, T. C. *J. Am. Chem. Soc*. **1988**, *110*, 7915.
(10) (a) Watson, P. *J. Am. Chem. Soc*. **1983**, *105*, 6491. (b) Fendrick, C. M.; Marks, T. J. *J. Am. Chem. Soc*. **1984**, *106*, 2214. (c) Fendrick, C. M.; Marks, T. J. *J. Am. Chem. Soc*. **1986**, *108*, 625. (d) Thompson, M. E.; Baxter, S. M.; Bulls, A. R.; Burger, B. J.; Nolan, M. C.; Santarsiero, B. D.; Schaefer, W. P.; Bercaw, J. E. *J. Am. Chem. Soc*. **1987**, *19*, 8109.
(11) Cummins, C. C.; Baxter, S. M.; Wolczanski, P. T. *J. Am. Chem. Soc*. **1988**, *110*, 8731.
(12) Periana, R. A.; Taube, D. J.; Evitt, E. R.; Lòffer, D. G.; Wentrcek, P. R.; Voss, G.; Masuda, T. *Science* **1993**, *259*, 340.

10.1021/ic0006302 CCC: $19.00
Published on Web 10/21/2000

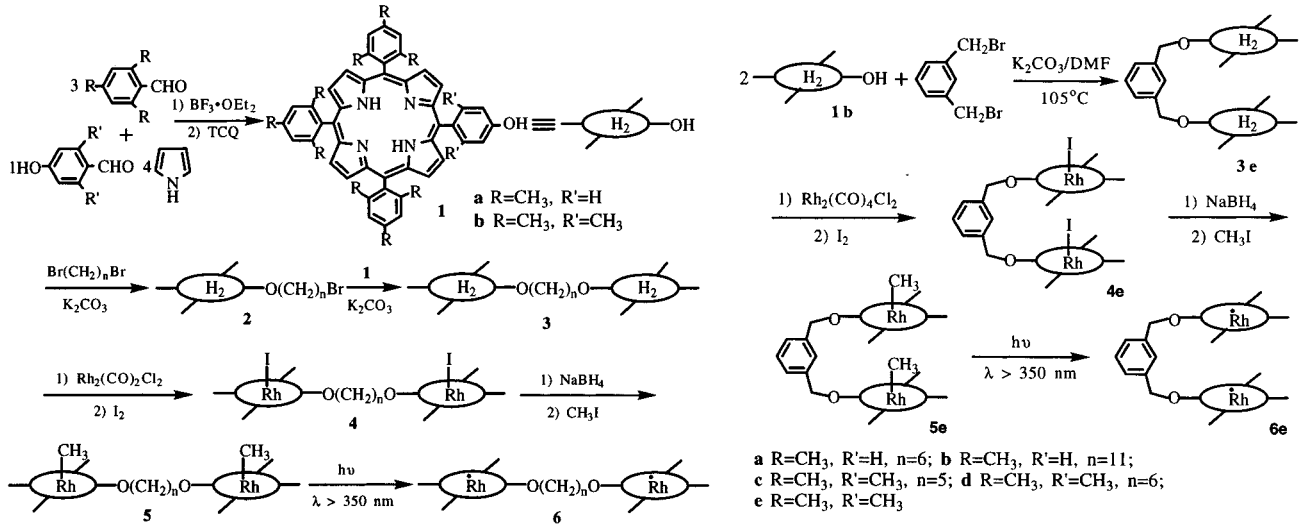

Figure 1. Schemes 1 and 2 for the preparation of diether-tethered diporphyrin ligands and the dirhodium(II) bimetalloradical derivatives.

that are used in forming dirhodium(II) porphyrin bimetalloradical species. Reactions of the diporphyrin bimetalloradical complexes with H_2 are used to illustrate the efficacy of this stategy.

Results and Discussion

A series of tethered diporphyrin ligands were designed specifically to improve the rates for rhodium(II) porphyrin reactions with substrates such as methane where two metalloradicals occur in the transition state. The two essential design features needed to accomplish this objective are the following: (1) The steric demands for the individual porphyrin units must be large enough to preclude intra- and intermolecular Rh(II)−Rh(II) bonding which makes an unfavorable contribution to the thermodynamics and kinetics of substrate reactions. (2) The length and flexibility of the tethering units must permit the two metal centers to reach the required transition state for intramolecular substrate reactions. These features have been incorporated into a set of diporphyrin ligands by linking two sterically demanding porphyrin units with a series of diether spacers through reactions of the *p*-hydroxy functionality on a phenyl group at the periphery of the porphyrin macrocycle (Figure 1, Schemes 1 and 2).

The first step in the construction of the target diporphyrins is to prepare porphyrins that have steric requirements similar to that of tetramesitylporphyrin ((TMP)H_2) and a functionality on the periphery for tethering the two porphyrin units. Synthesis of the functionalized sterically demanding porphyrins was accomplished by use of a combination of the Lindsey methodology[14] and a mixed aldehyde condensation approach. The condensation of mixtures of the desired aromatic aldehydes with pyrrole produced a near statistical mixture of meso-substituted porphyrins.

Condensation of 3 equiv of mesitaldehyde and 1 equiv of 4-hydroxybenzaldehyde or 2,6-dimethyl-4-hydroxybenzaldehyde with 4 equiv of pyrrole in the presence of $BF_3{\cdot}Et_2O$ (Figure 1, Scheme 1) resulted in the intermediate porphyrinogens which by oxidation with *p*-chloranil produced a porphyrin mixture that was separated by column chromatography. The first fraction was identified as tetramesitylporphyrin, (TMP)H_2. The second fraction afforded the desired functionalized steric porphyrin (TMP-OH)H_2 (**1a**) or (DMTMP-OH)H_2 (**1b**) in isolated yields of 16% and 14%, respectively.

Formation of dimeric porphyrins with different spacers from the functionalized steric porphyrins 1a,b was accomplished as described in Schemes 1 and 2 (Figure 1). Reactions of porphyrin **1a** or **1b** with an excess of α,ω-dibromoalkanes by nucleophilic substitution produced the bromoalkyl porphyrins (TMP-O$(CH_2)_n$-Br)H_2 (**2a**, $n = 6$; **2b**, $n = 11$) and (DMTMP-O$(CH_2)_n$Br)H_2 (**2c**, $n = 5$; **2d**, $n = 6$) in 74% to 83% yields. Subsequent reactions of the bromoalkyl porphyrins **2a**−**d** with an excess amount of the corresponding porphyrin **1** afforded the diporphyrin ligands H_2(por)O−X−O(por)H_2 (**3a**−**d**) in 55−65% yields. This stepwise synthesis of diporphyrins **3a**−**d** (Scheme 1) provides a potential approach for preparing heterobimetallodiporphyrins.[15,16] An alternate single step procedure for the synthesis of diporphyrin ligands is illustrated by the preparation of compound **3e** that contains a more rigid *m*-xylylene spacer (Scheme 2). Reaction of an excess amount of porphyrin **1a** with α,α'-dibromo-*m*-xylene in DMF afforded the diporphyrin **3e** in 87% yield.

Formation of Rhodium(II) Porphyrin Bimetalloradical. Rhodium is inserted in the diporphyrin ligands **3a**−**e** by reaction of $Rh_2(CO)_2Cl_2$[17] in 1,2-dichloroethane and then converted to the dimethyl derivatives H_3C−Rh(por)O−X−O(por)Rh−CH_3 **(5a**−**e)** in 80−85% isolated yields by the reaction sequence given in Schemes 1 and 2. The Rh−CH_3 groups in **5a**−**e** produce highly characteristic ^{1}H NMR because of the shielding effect from the aromatic porphyrin macrocycle and coupling

(13) (a) Crabtree, R. H. *Chem. Rev.* **1995**, *95*, 987. (b) Arndtsen, B. A.; Bergman, R. G.; Mobley, T. A.; Peterson, T. H. *Acc. Chem. Res.* **1995**, *28*, 154.

(14) (a) Lindsey, J. S.; Hsu, H. C.; Schreiman, I. C. *Tetrahedron Lett.* **1986**, *27*, 4969. (b) Lindsey, J. S.; Schreiman, I. C.; Hsu, H. C.; Marguerettaz, A. M. *J. Org. Chem.* **1987**, *52*, 827.

(15) (a) Guilard, R.; Lopez, M. A.; Tabard, A.; Richard, P.; Lecomte, C.; Brandes, S.; Hutchison, J.; Collman, J. P. *J. Am. Chem. Soc.* **1992**, *114*, 9877. (b) Collman, J. P.; Hutchison, J. E.; Lopez, M. A.; Tabard, A.; Guilard, R.; Seok, W. K.; Ibers, J. A.; L'Her, M. *J. Am. Chem. Soc.* **1992**, *114*, 9869. (c) Collman, J. P.; Wagenknecht, P. S.; Hutchison, J. E.; Lewis, N. S.; Lopez, M. A.; Guilard, R.; L'Her, M.; Bothner-By, A.; Mishra, P. K. *J. Am. Chem. Soc.* **1992**, *114*, 5654.

(16) (a) Tabushi, I.; Kugimiya, S.; Kinnaird, M. G.; Saaski, T. *J. Am. Chem. Soc.* **1985**, *107*, 4192. (b) Tabushi, I.; Saaski, T. *J. Am. Chem. Soc.* **1983**, *105*, 2901. (c) Tabushi, I.; Kugimiya, S.; Saaski, T. *J. Am. Chem. Soc.* **1985**, *107*, 5159. (d) Tabushi, I.; Kugimiya, S. *J. Am. Chem. Soc.* **1986**, *108*, 6926. (e) Tabushi, I. *Pure Appl. Chem.* **1988**, *60*, 581.

(17) (a) Ogoshi, H.; Setsune, J.; Omura, T.; Yoshida, Z. *J. Am. Chem. Soc.* **1975**, *97*, 6461. (b) Ogoshi, H.; Omura, T.; Yoshida, Z. *J. Am. Chem. Soc.* **1973**, *95*, 1666.

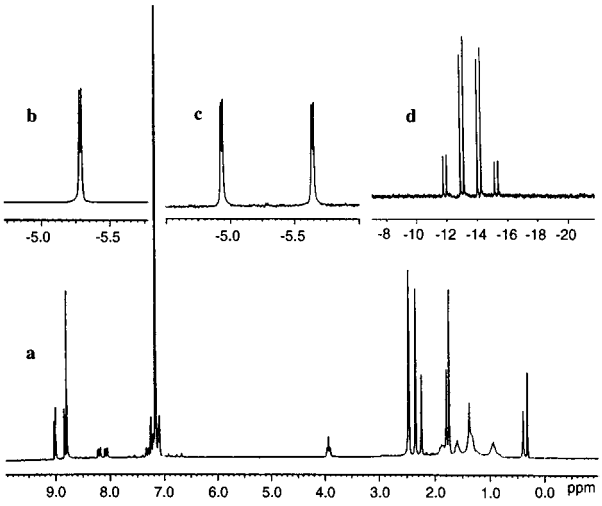

Figure 2. NMR spectra of $H_3C-Rh(por)O(CH_2)_6O(por)Rh-CH_3$ (5a) in C_6D_6: (a) ^1H NMR spectrum of diporphyrin unit; (b) ^1H NMR spectrum of $Rh-CH_3$ group; (c) ^1H NMR spectrum of $Rh-^{13}CH_3$ group; (d) proton-coupled ^{13}C NMR spectrum of $Rh-^{13}CH_3$ group.

from the ^{103}Rh nucleus. Distinctive high field positions for the ^1H and ^{13}C NMR spectrum of the $Rh-CH_3$ in $^{13}CH_3$–Rh-(por)O$-(CH_2)_6$–O(por)Rh$-^{13}CH_3$ (**5a**) ($\delta_{CH} = -5.29$; $\delta_{13CH} = -13.58$) and coupling ($^1J_{13C'H} = -141$ Hz; $^1J_{103Rh-13CH} = -29$ Hz; $^2J_{103Rh-CH} = 2.9$ Hz) (Figure 2) provide convenient observables for identifying the $Rh-CH_3$ derivative in solution.

Facile photohomolysis ($\lambda > 350$ nm) of the $Rh-CH_3$ units[1,2,18] in **5a**−**e** is an effective method to form dirhodium(II) bimetalloradical complexes (·Rh^{II}(por)O−X−O(por)Rh^{II}·) **6a**−**e** (Schemes 1 and 2). The rhodium(II) complexes **6a**−**e** exhibit broad yet observable paramagnetically shifted ^1H NMR spectra. Temperature dependence for the pyrrole ^1H NMR shift for the dirhodium(II) complex **6a** (·Rh(por)O$-(CH_2)_6$–O(por)Rh^{II}·) is illustrated in Figure 3. The observed downfield shift for the pyrrole hydrogens of **6a** (δ_{pyr}(295 K) = 18.2) is consistent with a $(d_{xy}\ d_{xz,yz})^6\ (d_{z2})^1$ ground configuration placing positive spin density in the porphyrin σ donor orbitals. Curie paramagnetism for **6a** is demonstrated by the linear dependence of the pyrrole hydrogen shift with the inverse of temperature (δ_{pyr} vs T^{-1}) (Figure 3).[19] The observed Curie magnetic behavior clearly demonstrates the absence of detectable $Rh^{II}-Rh^{II}$ bonding down to 190 K in toluene. The EPR spectrum for **6a** in toluene glass (90 K) (Figure 4) shows g values ($g_\perp = 2.64$; $g_{11} = 1.90$) very close to that for (TMP)Rh^{II}· ($g_\perp = 2.65$; $g_{11} = 1.915$)[20] resulting from effectively independent Rh^{II} centers with $(d_{xy}\ d_{xz,\ yz})^6\ (d_{z2})^1$ electron configurations. The broadening of the EPR spectrum which obscures the ^{103}Rh coupling on the g_{11} transition of the dirhodium(II) complex **6a** relative that for (TMP)Rh· ($A[^{103}Rh(g_{11})] = -197$ MHz) may result from a small magnetic interaction between the two rhodium(II) centers in the toluene glass.

Triphenylphosphine coordinates with the rhodium(II) centers of the bimetalloradical **6a** and exhibits an anisotropic EPR spectrum in toluene glass (90 K) associated with a di mono triphenyl phosphine adduct (Figure 4b). The g values ($g_\perp = 2.17$, $g_{11} = 2.00$) and hyperfine couplings ($A(^{31}P)g_\perp = 756$ MHz, $A(^{31}P)g_{11} = 1016$ MHz, $A(^{103}Rh)g_{11} = 61$ MHz) are similar to those observed for (TMP)Rh·P$(C_6H_5)_3$[20] and indicative of an $(d_{xz}d_{yz}\ d_{xy})^6\ (d_{z2})^1$ electron configuration with substantial odd electron spin density on the phosphine ligand. The triphenylphosphine adduct reacts with dioxygen ($Po_2 \sim 200-600$ Torr) to form a disuperoxo complex (Figure 4c) with the anisotropic EPR spectrum exhibiting three distinct g values ($g_1 = 2.08$, $g_2 = 2.005$, $g_3 = 1.996$) associated with low symmetry (por)Rh(III)$-O_2^-$ unit (Figure 4c). The small g value anisotropy and near isotropic phosphorus couplings ($\langle A\ (^{31}P)\rangle = 50.5$ MHz) are characteristic of superoxide complexes where the unpaired electron is predominantly localized on the dioxygen unit.

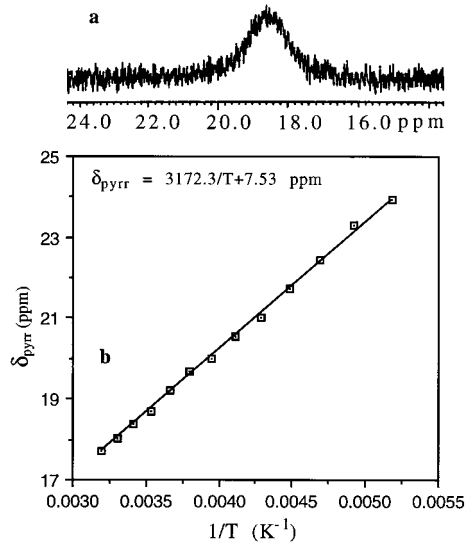

Figure 3. (a) ^1H NMR spectrum in the pyrrole region for ·Rh(Por)O-$(CH_2)_6$O(Por)Rh· (**6a**) in C_6D_6. (b) Temperature dependence for the pyrrole ^1H NMR paramagnetic shift of **6a** in toluene-d_8, displayed as a plot of chemical shift, δ (ppm), versus $1/T$ (K^{-1}).

Dirhodium(II) Bimetalloradical Reactions with Hydrogen. The dirhodium(II) bimetalloradical complexes (·Rh(por)O−X−O(por)Rh·) **6a**−**e** react with hydrogen ($P_{H2} = 540$ Torr; $T = 296-353$ K) in benzene to form the dihydride complex H−Rh-(por)O−X−O(por)Rh−H (**7a**−**e**). Throughout the above range of conditions each of these reactions effectively results in the quantitative conversion of the bimetalloradicals (**6**) into dihydride species (**7**).

The reaction of H_2 with the bimetalloradical complexes could proceed by either an intramolecular or intermolecular use of two Rh^{II}· centers to give bimolecular and termolecular processes, respectively (Figure 5). The termolecular pathway shown in Figure 5 is effectively the same as that used by (TMP)Rh· in the reaction with H_2.[3] The intramolecular reaction two Rh^{II}· centers in **6** with H_2 initially produces the same dihydride **7** which is the same hydride species that is present when the reaction is complete. However, when Rh^{II}· centers from two different molecules of **6** react with H_2, the product that initially forms has one Rh−H and one Rh^{II}· site in the molecule (compound **8**). Formation of the dihydride **7** by the intermolecular pathway thus would pass through an intermediate species **8**. More detailed reactivity studies of the bimetalloradical species **6a** and the dihydride **7a** were undertaken in an effort to distinguish between intra- and intermolecular pathways by both kinetic studies and observing the time evolution of reaction products.

The substantial rate enhancement for the reaction of the bimetalloradical 6a with H_2 compared to (TMP)Rh^{II}· is illustrated in Figure 6. Plots of the disappearance of Rh^{II}· centers

(18) (a) Wayland, B. B.; Sherry, A. E.; Poszmik, G.; Bunn, A. G. *J. Am. Chem. Soc*. **1992**, *114*, 1673. (b) Sherry, A. E.; Wayland, B. B. *J. Am. Chem. Soc.* **1989**, *111*, 5010.
(19) Drago, R. S. *Physical Methods for Chemists*, 2nd ed.; Saunders College Publishing: Philadelphia, PA, 1992; Chapter 12, p 508.
(20) Wayland, B. B.; Sherry, A. E.; Bunn, A. G. *J. Am. Chem. Soc*. **1993**, *115*, 7675.

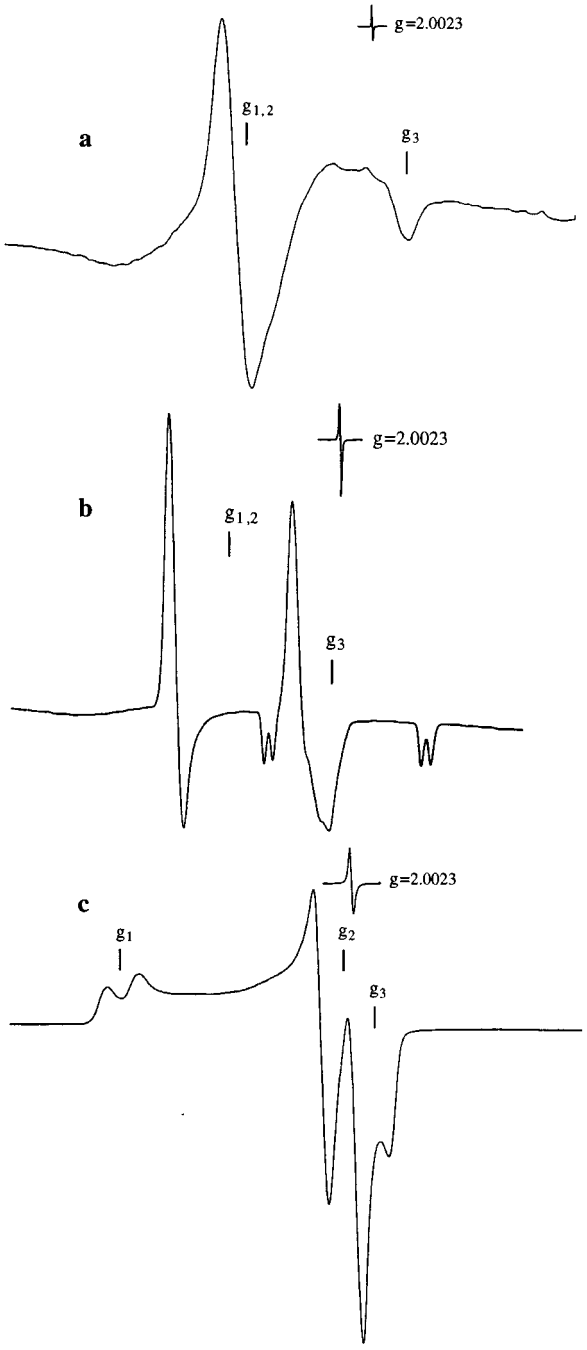

Figure 4. (a) Anisotropic EPR spectrum for ·Rh(Por)O(CH_2)$_6$O(Por)-Rh· (6a) (toluene glass, 90 K): $g_{1,2} = 2.64$, $g_3 = 1.90$. (b) Anisotropic EPR spectrum for the triphenyl phosphine adduct of **6a** (toluene glass, 90 K): $g_{1,2} = 2.17$, $A(^{31}P)g_{1,2} = 756$ MHz; $g_3 = 2.00$, $A(^{31}P)g_3 = 1016$ MHz, $A(^{103}Rh)g_3 = 61$ MHz. (c) Anisotropic EPR spectrum for the superoxo complex of the bis(triphenyl phosphine) adduct of **6a** (toluene glass, 90 K): $g_1 = 2.080$, $A(^{31}P)g_1 = 50.9$ MHz; $g_2 = 2.005$, $A(^{31}P)g_2 = 50.5$ MHz; $g_3 = 1.996$, $A(^{31}P)g_3 = 50.3$ MHz.

as a function of time for the reactions of the dirhodium(II) complex 6a and (TMP)Rh^{II}· with H_2 in C_6D_6 (296 K) are shown in Figure 6. The kinetics for the reaction of **6a** with H_2 are fitted to a bimolecular process with a second-order rate constant of 9.3×10^{-1} M^{-1} s^{-1} ($T = 296$ K) (Figure 7). The disappearance of (TMP) Rh^{II}· by reaction with H_2 as a function of time at the same concentration and temperature as the reaction of **6a** is calculated and plotted in Figure 6 using the previously determined third-order rate constant of 2.7 M^{-2} s^{-1} at 296 K.[1] The large increase in the rate of reaction of **6a** with H_2 compared to (TMP)Rh^{II}· and the fitting of the concentration−time profile

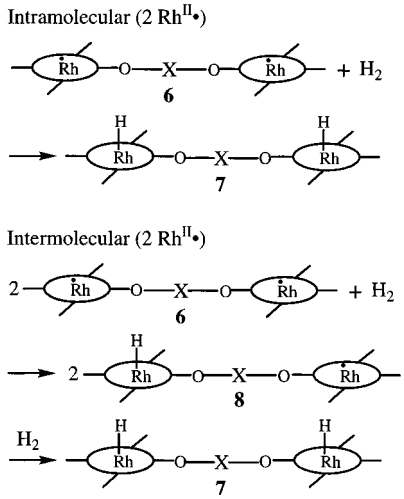

Figure 5. Sequence of hydride complexes formed by intramolecular and intermolecular reactions of two Rh^{II}· centers with H_2.

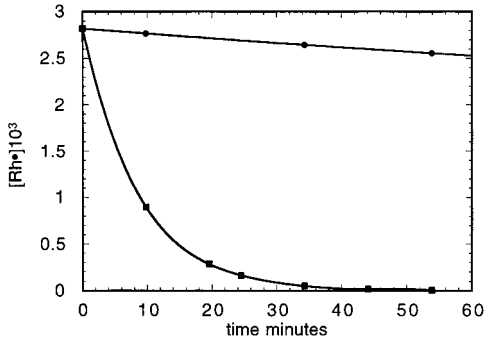

Figure 6. Change in the [Rh^{II}·] centers with time for reactions of hydrogen ([H_2] = 2.1×10^{-3} M) with (TMP)Rh^{II}· ($k(296) = 2.7$ M^{-1} s^{-1}) and ·Rh(por)(CH_2)$_6$O(por)Rh· (6a) ($k(296) = 9.3 \times 10^{-3}$ M^{-1} s^{-1}) at 296 K ([(TMP)]$_i = 2.82 \times 10^{-3}$ M; [**6a**]$_i = 1.41 \times 10^{-3}$ M, [Rh^{II}·]$_i$ (**6a**) $= 2.82 \times 10^{-3}$ M).

to a second-order process provide convincing evidence that the most productive path for the reaction of **6a** with H_2 involves the intramolecular use of two Rh^{II}· centers.

Additional direct evidence for the intramolecular path was obtained by observing the sequence of Rh−H species formed in the reactions of 6a with H_2 at low concentration. When a benzene solution of the bimetalloradical **6a** is put in contact with a low pressure of H_2 such that there is less than a stoichiometric amount of H_2 for the complete reaction ($P_{H_2i} \sim$ 3 Torr) the ^{1}H NMR spectrum of the Rh−H region observed over an extended period of time reveals a sequence of rhodium hydride species (Figure 7). The initially formed hydride complex has a ^{1}H NMR spectrum identical with that of the dihydride **7a**. After a period of several days a second hydride species appears and builds up in concentration with the decline in concentration of **7a**. We ascribe these observations to a relatively fast initial bimolecular reaction of **6a** with H_2 to produce the dihydride **7a** in a single step followed by a slower intermolecular hydrogen atom transfer from **7a** to **6a** to produce **8a** (·Rh-(por)O−(CH_2)$_{6-}$O(por)Rh−H) (Figure 8). Degenerate hydrogen atom transfer between (OEP)Rh−H and (OEP)Rh· is relatively fast but this type of process is much slower for the (TMP)Rh^{II}· system where the ligand steric demands inhibit attaining the transition state for atom transfer.

The ligand steric demands designed into the bimetalloradical radical complexes are similar to that of TMP and thus relatively slow intermolecular hydrogen atom transfer is expected between **6a** and **7a**. Support for this interpretation was obtained from a

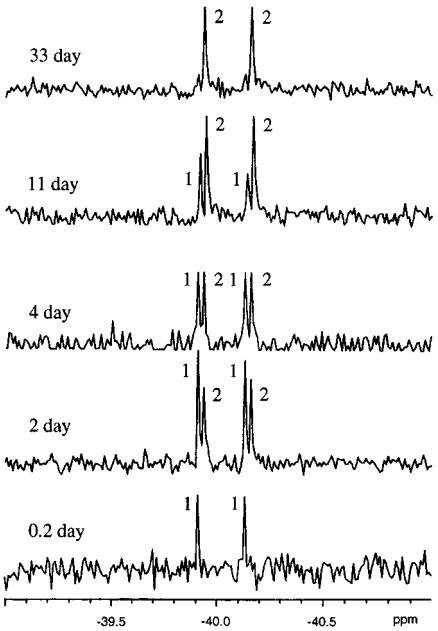

Figure 7. Sequence of ^{1}H NMR for the ^{103}Rh−H region for C_6D_6 solutions for **6a** exposed to a small initial pressure of H_2 (P_{H2i} = 3 Torr).

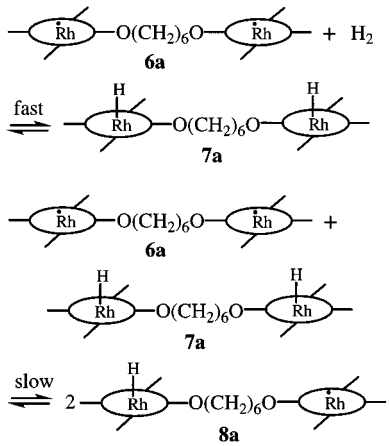

Figure 8. Sequence of Rh−H species formed when a C_6D_6 solutions of 6a reacts with a less than stoichiometric quantity of H_2. The dihydride **7a** forms first, and then is slowly converted to a second hydride species **8a**.

separate experiment where isolated samples of the dihydride **7a** and bimetalloradical **6a** were mixed in C_6D_6 solvent. The initial ^{1}H NMR spectrum obtained by mixing **6a** and **7a** was that of the dihydride **7a**, but a second hydride species with ^{1}H NMR identical with **8a** grew in over a period of days. The sequence of hydride species formed in the reaction of **6a** with H_2 clearly indicates that the intramolecular reaction of two Rh^{II}· centers with H_2 has a large kinetic preference compared to the intermolecular pathway where Rh^{II}· centers in two molecules of **6a** are used. Both kinetic studies and the sequence of Rh−H species formed indicate that the reaction of the bimetalloradical complex **6a** with dihydrogen occurs through a bimolecular process that involves the intramolecular use of two Rh^{II}· centers.

Experimental Section

General Procedures and Methods. All manipulations were performed on a high-vacuum line equipped with a Welch Duo-Seal vacuum pump or in an inert-atmosphere box filled with argon unless otherwise noted. All reagents were purchased from Aldrich or Strem Chemical Co. and used as received. Pyrrole was distilled prior to use. $[Rh(CO)_2Cl]_2$ was sublimed prior to use. Deuterated NMR solvents such as benzene and toluene were degassed by freeze−pump−thaw cycles to remove oxygen and then refluxed over sodium/benzophenone ketyl to remove water as indicated by turning purple. Chloroform, methylene chloride, and 1,2-dichloroethane used in synthetic procedures were purified by washing three times with water followed by chromatography on grade 1 alumina for the removal of ethanol and water. Prepurified nitrogen and argon gases used for the inert-atmosphere box were purchased from Airco or MG industries.

Proton NMR spectra were obtained on a Bruker WP200SY, a Bruker AC-250, or a Bruker AMX-500 interfaced to an Aspect 300 computer at ambient temperature. All spectra were referenced using the residual solvent peak as an internal standard (benzene-d_6, δ = 7.155; toluene-d_8, δ = 2.09; chloroform-d_1, δ = 7.24). Carbon-13 NMR spectra were obtained on the AMX-500 instrument equipped with a carbon-13 probe. Variable-temperature ^{1}H NMR spectra were obtained on an IBM-Bruker AF200SY or IBM Bruker WP200SY spectrometer equipped with a Bruker VI-1000 temperature controller or boil-off from liquid nitrogen when temperature needed is below 220 K. The probe was cooled with a FTS systems refrigerator unit equipped with a temperature controller. The temperatures in the probe were referenced against an external samples of methanol and ethylene glycol for low- and high-temperature experiments, respectively. The samples were protected from light prior to and during the experiments.

Electron paramagnetic resonance spectra were obtained by use of ER 100 D X-band spectrometer. Temperature measurements were calibrated with a Bruker model VT unit using N_2 as the cooling source (283−90 K). All EPR experiments were performed at 90 K unless otherwise noted and calibrated using diphenylpicrylhydrazine (DPPH, $\langle g \rangle$ = 2.0036) as an external standard. Fast atom bombardment mass spectrometry (FAB-MS) data were recorded on a VG-ZAB-E spectrometer with a cesium ion gun. Electronic spectra were recorded with a Hewlett-Packard UV 8452 instrument interfaced to an IBM PC.

5-(4-Hydroxyphenyl)-10,15,20-trimesitylporphyrin, (TMP-OH)-H_2 (1a). A 2 L three-neck round-bottomed flask fitted with a septum, reflux condenser, and nitrogen inlet port was charged with $CHCl_3$ (1 L) (distilled from K_2CO_3), 4-hydroxybenzaldehyde (305 mg, 2.5 mmol), mesitaldehyde (1.106 mL, 7.5 mmol), and pyrrole (694 μL, 10 mmol). After the solution was purged with N_2 for 5 min, BF_3·OEt_2 (1.32 mL) was added via syringe. The room-temperature reaction was monitored by removing 50-mL aliquots and oxidizing with excess *p*-chloranil, followed by UV−vis absorption spectroscopy. At the end of 60 min, *p*-chloranil (1.844 g, 7.5 mmol) was added in powder form and the reaction mixture was gently refluxed (~60 °C) for 1 h. The reaction mixture was then cooled to room temperature, and the precipitates were filtered off. The filtrate was rotary evaporated to dryness under reduced pressure. The crude dry product was purified by column chromatography on silica gel with chloroform first and then with dichloromethane as eluents. The first fraction was identified as $(TMP)H_2$. The second fraction was evaporated and dried to give **1a** as a purple solid in 16% yield. ^{1}H NMR (C_6D_6), δ (ppm): 8.92 (d, 2H, $^3J_{H-H}$ = 4.8 Hz, pyrrole), 8.85 (d, 2H, $^3J_{H-H}$ = 4.8 Hz, pyrrole), 8.84 (d, 2H, $^3J_{H-H}$ = 4.8 Hz, pyrrole), 8.82 (d, 2H, $^3J_{H-H}$ = 4.8 Hz, pyrrole), 7.78 (d, 2H, $^3J_{H-H}$ = 8.2 Hz, *o*-phenyl), 7.11 (s, 6H, *m*-phenyl), 6.42 (d, 2H,$^3J_{H-H}$ = 8.2 Hz, m′-phenyl), 4.25 (br s, 1H, −OH), 2.45 (s, 6H, *p*-CH_3), 2.41 (s, 3H, p′-CH_3), 1.96 (s, 12H, *o*-CH_3), 1.84 (s, 6H, o′-CH_3), −1.73 (br s, 2H, −NH). UV−vis (CH_2Cl_2), λ_{max} (nm): 650, 592, 548, 514, 414. FAB-HRMS (M^+): calcd for $C_{53}H_{48}N_4O$, *m*/*e* 756.3829; found, *m*/*e* 756.3894.

5-(2,6-Dimethyl-4-hydroxyphenyl)-10,15,20-trimesitylporphyrin, (DMTMP-OH)H_2 (1b). The porphyrin **1b** was prepared in 14% yield by a procedure analogous to that given for porphyrin **1a** using 2,6-dimethyl-4-hydroxybenzaldehyde instead of 4-hydroxybenzaldehyde. ^{1}H NMR (C_6D_6), δ (ppm): 8.81 (s, 4H, pyrrole H), 8.79 (s, 4H, pyrrole H), 7.13 (s, 4H, arom), 6.59 (s, 4H, arom), 4.12 (broad s, 1H, −OH), 2.43 (s, 9H, *p*-CH_3), 1.89 (s, 18H, *o*-CH_3), 1.79 (s, 6H, *o*-CH_3), −1.64 (broad s, 2H, −NH). UV−vis (CH_2Cl_2), λ_{max} (nm): 646, 592, 546, 514, 416. FAB-HRMS (M^+): calcd for $C_{55}H_{52}N_4O$, *m*/*e* 784.4141; found, *m*/*e* 784.4076.

5-[4-(6-Bromo-1-hexoxy)phenyl]-10,15,20-trimesitylporphyrin, [TMP-O$(CH_2)_6$Br]H_2 (2a). A mixture of porphyrin **1a** (635 mg, 0.84 mmol), 1,6-dibromohexane (1.72 mL, 11.16 mmol), and anhydrous K_2-

CO_3 (1.69 g, 12.23 mmol) was magnetically stirred with DMF (17 mL, dried over 4 Å molecular sieves). The reaction was monitored by TLC (silica gel, CH_2Cl_2). After 30 h, the reaction mixture was rotary evaporated to dryness under reduced pressure. A mixture of water (96 mL) and methanol (17 mL) was added to treat the residue. Upon centrifuging of the sample, the precipitates were collected and dried in vacuo at 100 °C to remove excess 1,6-dibromohexane and then purified by column chromatography (silica gel, CH_2Cl_2) to give porphyrin **2a** in 83% yield. ^{1}H NMR (C_6D_6), δ (ppm): 9.02 (d, 2H, $^3J_{H-H}$ = 4.8 Hz, pyrrole), 8.88 (d, 2H, $^3J_{H-H}$ = 4.8 Hz, pyrrole), 8.87 (d, 2H, $^3J_{H-H}$ = 4.8 Hz, pyrrole), 8.83 (d, 2H, $^3J_{H-H}$ = 4.8 Hz, pyrrole), 7.96 (d, 2H, $^3J_{H-H}$ = 8.5 Hz, *o*-phenyl), 7.16 (s, 6H, *m*-phenyl), 7.10 (d, 2H, $^3J_{H-H}$ = 8.5 Hz, m′-phenyl), 3.74 (t, 2H, $^3J_{H-H}$ = 6.3 Hz, $-OCH_{2-}$), 2.98 (t, 2H, $^3J_{H-H}$ = 6.7 Hz, $-CH_2Br$), 2.45 (s, 6H, *p*-CH_3), 2.41 (s, 3H, *p*′-CH_3), 1.97 (s, 12H, *o*-CH_3), 1.85 (s, 6H, o′-CH_3), 1.55−1.16 (m, 8H, $-CH_2CH_2CH_2CH_{2-}$), −1.69 (br s, 2H, −NH). UV−vis (CH_2Cl_2), λ_{max} (nm): 650, 592, 548, 516, 418. FAB-HRMS (M^+): calcd for $C_{59}H_{59}N_4$OBr, *m*/*e* 918.3837; found, *m*/*e* 918.3840.

5-[4-(11-Bromo-1-undecoxy)phenyl]-10,15,20-trimesitylporphyrin, [TMP-O(CH$_2$)$_{11}$Br]H$_2$ (2b). The porphyrin **2b** was prepared in 80% yield by a procedure analogous to that given for porphyrin **2a** using 1,11-dibromoundecane instead of 1,6-dibromohexane. ^{1}H NMR (C_6D_6), δ (ppm) 9.02 (d, 2H, $^3J_{H-H}$ = 4.8 Hz, pyrrole), 8.88 (d, 2H, $^3J_{H-H}$ = 4.8 Hz, pyrrole), 8.87 (d, 2H, $^3J_{H-H}$ = 4.8 Hz, pyrrole), 8.83 (d, 2H, $^3J_{H-H}$ = 4.8 Hz, pyrrole), 7.96 (d, 2H, $^3J_{H-H}$ = 8.5 Hz, *o*-phenyl), 7.16 (s, 6H, *m*-phenyl), 7.11 (d, 2H, $^3J_{H-H}$ = 8.5 Hz, *m*′-phenyl), 3.86 (t, 2H, $^3J_{H-H}$ = 6.2 Hz, $-OCH_{2-}$), 2.99 (t, 2H, $^3J_{H-H}$ = 6.7 Hz, $-CH_2Br$), 2.45 (s, 6H, *p*-CH_3), 2.42 (s, 3H, *p*′-CH_3), 1.97 (s, 12H, *o*-CH3), 1.85 (s, 6H, *o*′-CH_3), 1.55−1.16 (m, 8H, $-(CH_2)_{9-}$), −1.68 (br s, 2H, −NH). UV−vis (CH_2Cl_2), λ_{max} (nm): 646, 592, 547, 514, 416. FAB-HRMS (M^+): calcd for $C_{59}H_{59}N_4$Obr, *m*/*e* 918.3837; found, *m*/*e* 918.3840.

5-[4-(5-Bromo-1-pentoxy)-2,6-dimethylphenyl]-10,15,20-trimesitylporphyrin, [DMTMP-O(CH$_2$)$_5$Br]H$_2$ (2c). The porphyrin **2c** was prepared in 74% yield by a procedure analogous to that given for porphyrin **2a** using porphyrin **1b** and 1,5-dibrompentane instead of porphyrin **1a** and 1,6-dibromohexane. ^{1}H NMR ($CDCl_3$), δ (ppm): 8.63 (s, 4H, pyrrole H), 8.62 (s, 4H, pyrrole H), 7.27 (s, 6H, arom), 7.00 (s, 2H, arom), 4.24 (t, 2H, $^3J_{H-H}$ = 6.1 Hz, $-CH_2O$), 3.54 (t, 2H, $^3J_{H-H}$ = 6.7 Hz, $-CH_2Br$), 2.62 (s, 9H, *p*-CH_3), 1.95−2.10 (m, 6H, $-CH_2CH_2CH_{2-}$), 1.86 (s, 24H, *o*-CH_3), −2.52 (s, 2H, −NH). UV−vis (CH_2Cl_2), λ_{max} (nm): 646, 592, 548, 514, 416. FAB-HRMS (M^+): calcd for $C_{60}H_{61}N_4$Obr, *m*/*e* 932.4030; found, *m*/*e* 932.4061.

5-[4-(6-Bromo-1-hexoxy)-2,6-dimethylphenyl]-10,15,20-trimesitylporphyrin, [DMTMP-O(CH$_2$)$_6$Br]H$_2$ (2d). The porphyrin **2d** was prepared in 75% yield using porphyrin **1b** instead of **1a** by a procedure analogous to that given for the porphyrin **2a**. ^{1}H NMR (C_6D_6), δ (ppm): 8.88 (d, 2H, $^3J_{H-H}$ = 4.7 Hz, pyrrole), 8.83 (d, 2H, $^3J_{H-H}$ = 4.7 Hz, pyrrole), 8.82 (s, 4H, pyrrole), 7.13 (s, 6H, *m*-phenyl), 7.06 (s, 2H, *m*′-phenyl), 3.84 (t, 2H, $^3J_{H-H}$ = 6.2 Hz, $-OCH_{2-}$), 3.00 (t, 2H, $^3J_{H-H}$ = 6.7 Hz, $-CH_2Br$), 2.42 (s, 9H, *p*-CH_3), 1.90 (s, 24H, *o*-CH_3), 1.67−1.25 (m, 8H, $-CH_2CH_2CH_2CH_{2-}$), −1.63 (br s, 2H, −NH). UV−vis (CH_2Cl_2), λ_{max} (nm): 646, 592, 546, 514, 416. FAB-HRMS (M^+): calcd for $C_{61}H_{63}N_4$OBr, *m*/*e* 946.4183; found, 946.4149.

5,10,15-Trimesityl-20-[4-[6-(*p*-(10,15,20-trimesityl-5-porphinyl)-phenoxy)he xoxy]phenyl]porphine, H$_2$[TMP-O(CH$_2$)$_6$O-TMP]H$_2$ (3a). A mixture of **1a** (293 mg, 0.387 mmol) and porphyrin **2a** (119 mg, 0.129 mmol) were stirred with anhydrous K_2CO_3 (640 mg, 4.63 mmol) in DMF (10 mL). The reaction was monitored by TLC (silica gel, toluene/petroleum ether (v/v) = 2.5/1). After 28 h, the reaction mixture was evaporated under reduced pressure to dryness and treated with dichloromethane and water to remove inorganic salts. The organic layer was concentrated in vacuo and purified by column chromatography (silica gel, toluene/petroleum ether (v/v) = 2.5/1). The second fraction was identified as diporphyrin **3a** and obtained in 65% yield. ^{1}H NMR (C_6D_6), δ (ppm): 9.04 (d, 4H, $^3J_{H-H}$ = 4.8 Hz, pyrrole), 8.89 (d, 4H, $^3J_{H-H}$ = 4.8 Hz, pyrrole), 8.86 (d, 4H, $^3J_{H-H}$ = 4.8 Hz, pyrrole), 8.83 (d, 4H, $^3J_{H-H}$ = 4.8 Hz, pyrrole), 7.98 (d, 4H, $^3J_{H-H}$ = 8.5 Hz, *o*-phenyl), 7.18 (s, 12H, *m*-phenyl), 7.14 (d, 4H,$^3J_{H-H}$ = 8.5 Hz, *m*′-phenyl), 3.88 (t, 4H, $^3J_{H-H}$ = 6.1 Hz, $-OCH_{2-}$), 2.45 (s, 12H, *p*-CH_3), 2.41 (s, 6H, *p*′-CH_3), 1.97 (s, 24H, *o*-CH_3), 1.85 (s, 12H, o′-CH_3), 1.54−1.36 (m, 8H, $-CH_2CH_2CH_2CH_{2-}$), −1.68(br s, 4H, −NH). UV−vis (CH_2Cl_2), λ_{max} (nm): 648, 592, 548, 514, 418. FAB-HRMS (M^+): calcd for $C_{112}H_{106}N_8O_2$, *m*/*e* 1594.8441; found, *m*/*e* 1594.8312.

5,10,15-Trimesityl-20-[4-[11-[*p*-(10,15,20-trimesityl-5-porphinyl)-phenoxy]u ndecoxy]phenyl]porphine, H$_2$[TMP-O(CH$_2$)$_{11}$O-TMP]-H$_2$ (3b). The diporphyrin **3b** was prepared in 63% yield from the reaction of porphyrin **1a** with **2b** by a procedure analogous to that given for diporphyrin **3a**. ^{1}H NMR (C_6D_6), δ (ppm): 9.02 (d, 4H, $^3J_{H-H}$ = 4.8 Hz, pyrrole), 8.88 (d, 4H, $^3J_{H-H}$ = 4.8 Hz, pyrrole), 8.87 (d, 4H, $^3J_{H-H}$ = 4.8 Hz, pyrrole), 8.83 (d, 4H, $^3J_{H-H}$ = 4.8 Hz, pyrrole), 7.97 (d, 4H, $^3J_{H-H}$ = 8.5 Hz, *o*-phenyl), 7.16 (s, 12H, *m*-phenyl), 7.12 (d, 4H, $^3J_{H-H}$ = 8.5 Hz, *m*′-phenyl), 3.88 (t, 4H, $^3J_{H-H}$ = 6.1 Hz, $-OCH_{2-}$), 2.44 (s, 12H, *p*-CH_3), 2.42 (s, 6H, *p*′-CH_3), 1.97 (s, 24H, *o*-CH_3), 1.85 (s, 12H, o′-CH_3), 1.54−1.36 (m, 8H, $-(CH_2)_{9-}$), −1.68(br s, 4H, −NH). UV−vis (CH_2Cl_2) λ_{max} (nm): 645, 591, 548, 514, 416. FAB-HRMS (MH^+): calcd for $C_{117}H_{116}N_8O_2$, *m*/*e* 1665.9301; found, *m*/*e* 1665.9358.

5,10,15-Trimesityl-20-[4-[5-[*p*-(10,15,20-trimesityl-5-porphinyl)-2,6-dimeth ylphenoxy]pentoxy]-2,6-dimethylphenyl]porphine, H$_2$-[DMTMP-O (CH$_2$)$_5$O-DMTMP]H$_2$ (3c). The diporphyrin **3c** was prepared in 55% yield from the reaction of porphyrin **1b** with **2c** by a procedure analogous to that given for diporphyrin **3a**. ^{1}H NMR ($CDCl_3$) δ (ppm): 8.65 (d, 4H, $^3J_{H-H}$ = 4.7 Hz, pyrrole), 8.62 (d, 4H, $^3J_{H-H}$ = 4.7 Hz, pyrrole), 8.61 (s, 8H, pyrrole),7.25 (s, 12H, arom), 7.05 (s, 4H, arom), 4.34 (t, 4H, $^3J_{H-H}$ = 5.8 Hz, $-CH_2O$), 2.60 (s, 18H, *p*-CH_3), 2.16 (m, 6H, $-CH_2CH_2CH_{2-}$), 1.87 (s, 12H, *o*-CH_3), 1.84 (s, 36H, *o*′-CH_3), −2.52 (s, 4H, −NH). UV−vis (CH_2Cl_2), λ_{max} (nm): 646, 592, 546, 514, 414. FAB-HRMS (M^+): calcd for $C_{115}H_{112}N_8O_2$, *m*/*e* 1636.8910; found, *m*/*e* 1636.8921.

5,10,15-Trimesityl-20-[4-[6-[*p*-(10,15,20-trimesityl-5-porphinyl)-2,6-dimeth ylphenoxy]hexoxy]-2,6-dimethylphenyl]porphine, H$_2$-[DMTMP-O(CH$_2$)$_6$O-DMTMP]H$_2$ (3d). The diporphyrin **3d** was prepared in 60% yield from the reaction of porphyrin **1b** with **2d** by a procedure analogous to that given for diporphyrin **3a**. ^{1}H NMR (C_6D_6), δ (ppm): 8.89 (d, 4H, $^3J_{H-H}$ = 4.7 Hz, pyrrole), 8.83 (d, 4H, $^3J_{H-H}$ = 4.7 Hz, pyrrole), 8.82 (s, 8H, pyrrole), 7.13 (s, 16H, *m*-phenyl), 3.98 (t, 4H, $^3J_{H-H}$ = 6.1 Hz, $-OCH_{2-}$), 2.42 (s, 18H, *p*-CH_3), 1.93 (s, 12H, *o*-CH_3), 1.90 (s, 36H, *o*′-CH_3), 1.66−1.45 (m, 8H, $-CH_2CH_2CH_2CH_{2-}$), −1.62(br s, 4H, −NH). UV−vis (CH_2Cl_2), λ_{max} (nm): 646, 590, 546, 514, 418. FAB-HRMS (M^+): calcd for $C_{116}H_{114}N_8O_2$, *m*/*e* 1650.9067; found, *m*/*e* 1650.8982.

5,10,15-Trimesityl-20-[4-[α,α′-[*p*-(10,15,20-trimesityl-5-porphinyl)-phenoxy] xyloxy]phenyl]porphine, H$_2$[TMP-O(*m*-CH$_2$C$_6$H$_4$CH$_2$)O-TMP]H$_2$ (3e). A mixture of porphyrin **1a** (225 mg, 0.297 mmol) and α,α′-dibromo-*m*-xylene (39 mg, 0.149 mmol) was stirred with anhydrous K_2CO_3 (406 mg, 2.94 mmol) in DMF (20 mL) at 110 °C. The reaction was monitored by TLC (silica gel, toluene/petroleum ether (v/v) = 2.5/1). After 24 h, the reaction mixture was poured into a solvent mixture containing water (90 mL) and methanol (10 mL). The precipitates were filtered off using a Buchner funnel (type D) and washed with a small amount of methanol. The residue was dried in an oven at 100 °C and was purified by column chromatography (silica gel, toluene/petroleum ether (v/v) = 2.5/1). The second fraction was identified as diporphyrin **3e** and obtained in 87% yield. ^{1}H NMR (C_6D_6), δ (ppm): 9.02 (d, 4H, $^3J_{H-H}$ = 4.7 Hz, pyrrole), 8.89 (d, 4H, $^3J_{H-H}$ = 4.7 Hz, pyrrole), 8.85 (d, 4H, $^3J_{H-H}$ = 4.7 Hz, pyrrole), 8.83 (d, 4H, $^3J_{H-H}$ = 4.7 Hz, pyrrole), 7.97 (d, 4H, $^3J_{H-H}$ = 8.4 Hz, *o*-phenyl), 7.72−7.16 (multiple s, 16H, phenyl), 7.00 (d, 4H, $^3J_{H-H}$ = 8.4 Hz, *m*′-phenyl), 4.95 (s, 4H, $-OCH_{2-}$), 2.42 (s, 18H, *p*-CH_3), 1.98 (s, 24H, *o*-CH_3), 1.86 (s, 12H, o′-CH_3), −1.68 (br s, 4H, −NH). UV−vis (CH_2Cl_2), λ_{max} (nm): 645, 591, 548, 514, 418. FAB-HRMS (MH^+): calcd for $C_{114}H_{103}N_8O_2$, *m*/*e* 1615.8204; found, *m*/*e* 1615.8132.

I−Rh[TMP-O(CH$_2$)$_6$O-TMP]Rh−I (4a). In a three-neck flask fitted with a reflux condenser and an addition funnel, a solution of $[Rh(CO)_2Cl]_2$ (88 mg, 0.226 mmol) in dry 1,2-dichloroethane (10 mL) were added dropwise under argon to a suspension containing diporphyrin **3a** (52.4 mg, 0.033 mmol) and anhydrous NaOAc (44 mg, 0.536 mmol) in 1,2-dichloroethane (18 mL). The resulting reaction mixture was refluxed (∼80 °C) under argon for 48 h. After the mixture was cooled to room temperature, I_2 was added in two stages, 44 mg (0.173 mmol) initially and an additional 44 mg (0.173 mmol) after 2 h. The reaction mixture was stirred overnight at room temperature under argon.

Filtration and concetration gave a crude material which was treated with CH_2CI_2 and a saturated $Na_2S_2O_3$ aqueous solution for removal of excess iodine. The organic phase was concentrated and purified by column chromatography (silica gel, CH_2CI_2/hexane (v/v) = 5/1) to give iodorhodium(III) diporphyrin complex **4a** in 75% yield. ^{1}H NMR (C_6D_6), δ (ppm): 9.05 (d, 4H, $^3J_{H-H}$ = 4.9 Hz, pyrrole), 8.90 (d, 4H, $^3J_{H-H}$ = 4.9 Hz, pyrrole), 8.87 (s, 8H, pyrrole), 8.17 (dd, 2H, $^3J_{H-H}$ = 8.4 Hz, $^4J_{H-H}$ = 2.1 Hz, *o*-phenyl), 7.94 (dd, 2H, $^3J_{H-H}$ = 8.4 Hz, $^4J_{H-H}$ = 2.1 Hz, *o*′-phenyl), 7.28 (dd, 2H,$^3J_{H-H}$ = 8.4 Hz, $^4J_{H-H}$ = 2.6 Hz, *m*-phenyl), 7.10 (dd, 2H, $^3J_{H-H}$ = 8.4 Hz, $^4J_{H-H}$ = 2.6 Hz, *m*′-phenyl), 7.25 (s, 4H, *m*″-phenyl), 7.21 (s, 2H, *m*‴-phenyl), 7.09 (s, 2H, *m*⁗-phenyl), 7.05 (s, 4H, *m*⁗⁗-phenyl), 3.88 (t, 4H, $^3J_{H-H}$ = 6.1 Hz, $-OCH_{2-}$), 2.45 (s, 18H, *p*-CH_3), 2.37 (s, 12H, *o*-CH_3), 2.26 (s, 6H, *o*′-CH_3), 1.82 (s, 6H, *o*″-CH_3), 1.79 (s, 12H, *o*‴-CH_3), 2.01 (m, 4H, $-OCCH_{2-}$), 1.63 (m, 4H, $-CCH_2CH_2C-$). UV−vis ($CHCl_3$), λ_{max} (nm): 532, 420. FAB-MS for $C_{112}H_{102}N_8O_2Rh_2I_2$: *m*/*e* 2052 ($M^+$), 1925 ($M^+$ − I), 1798 (M^+ − 2I).

I−Rh[TMP-O$(CH_2)_{11}$O-TMP]Rh−I (4b). The iodorhodium(III) diporphyrin complex **4b** was prepared in 73% yield from diporphyrin **3b** by a procedure analogous to that given for complex **4a**. ^{1}H NMR (C_6D_6), δ (ppm): 9.06 (d, 4H, $^3J_{H-H}$ = 4.9 Hz, pyrrole), 8.91 (d, 4H, $^3J_{H-H}$ = 4.9 Hz, pyrrole), 8.89 (s, 8H, pyrrole), 8.20 (dd, 2H, $^3J_{H-H}$ = 8.4 Hz, $^4J_{H-H}$ = 2.1 Hz, *o*-phenyl), 7.92 (dd, 2H, $^3J_{H-H}$ = 8.4 Hz, $^4J_{H-H}$ = 2.1 Hz, *o*′-phenyl), 7.24 (dd, 2H, $^3J_{H-H}$ = 8.4 Hz, $^4J_{H-H}$ = 2.6 Hz, *m*-phenyl), 7. 07 (dd, 2H, $^3J_{H-H}$ = 8.4 Hz, $^4J_{H-H}$ = 2.6 Hz, *m*′-phenyl), 7.25 (s, 4H, *m*″-phenyl), 7.21 (s, 2H, *m*‴-phenyl), 7.09 (s, 2H, *m*⁗-phenyl), 7.05 (s, 4H, *m*⁗⁗-phenyl), 3.88 (t, 4H, $^3J_{H-H}$ = 6.1 Hz, $-OCH_{2-}$), 2.45 (s, 18H, *p*-CH_3), 2.33 (s, 12H, *o*-CH_3), 2.25 (s, 6H, *o*′-CH_3), 1.81 (s, 18H, *o*″-CH_3), 2.10 (m, 4H, $-OCCH_{2-}$), 1.55−1.32 (m, 14H, $-C(CH_2)_7C-$). UV−vis ($CHCl_3$), λ_{max} (nm): 530, 422. FAB-MS for $C_{117}H_{112}N_8O_2Rh_2I_2$: 1868 ($M^+$ − 2I).

I−Rh[DMTMP-O$(CH_2)_5$O-DMTMP]Rh−I (4c). The iodorhodium(III) diporphyrin complex **4c** was prepared in 70% yield from diporphyrin **3c** by a procedure analogous to that given for complex **4a**. ^{1}H NMR (C_6D_6), δ (ppm): 8.93 (d, 4H, $^3J_{H-H}$ = 4.9 Hz, pyrrole), 8.86 (d, 4H, $^3J_{H-H}$ = 4.9 Hz, pyrrole), 8.84 (s, 8H, pyrrole), 7.23, 7.08, 7.03 (three s, 16H, arom), 4.00 (t, 4H, $^3J_{H-H}$ = 6.1 Hz, $-CH_2O$), 2.44 (s, 18H, *p*-CH_3), 2.39, 2.36 (two s, 24H, *o*-CH_3), 2.16 (m, 6H, $-CH_2$-CH_2CH_{2-}), 1.80, 1.75 (two s, 24H, *o*-CH_3). UV−vis (CH_2Cl_2), λ_{max} (nm): 528, 420. FAB-MS for $C_{115}H_{108}N_8O_2Rh_2I_2$: *m*/*e* 2093 ($M^+$), 1965 ($M^+$ − I), 1838 (M^+ − 2I).

I−Rh[DMTMP-O$(CH_2)_6$O-DMTMP]Rh−I (4d). The iodorhodium(III) diporphyrin complex **4d** was in 65% yield prepared from diporphyrin **3d** by a procedure analogous to that given for complex **4a**. ^{1}H NMR (C_6D_6), δ (ppm): 8.87 (d, 4H, $^3J_{H-H}$ = 4.9 Hz, pyrrole), 8.84 (d, 4H, $^3J_{H-H}$ = 4.9 Hz, pyrrole), 8.81 (s, 8H, pyrrole), 7.23, 7.08, 7.03 (three s, 16H, arom), 4.00 (t, 4H, $^3J_{H-H}$ = 6.1 Hz, $-CH_2O$), 2.44 (s, 18H, *p*-CH_3), 2.39, 2.36 (two s, 24H, *o*-CH_3), 2.16 (m, 6H, $-CH_2$-CH_2CH_{2-}), 1.80, 1.75 (two s, 24H, *o*-CH_3). UV−vis (CH_2Cl_2), λ_{max} (nm): 529, 420. FAB-MS for $C_{116}H_{110}N_8O_2Rh_2I_2$: *m*/*e* 2107 ($M^+$), 1979 ($M^+$ − I), 1852 (M^+ − 2I).

I−Rh[TMP-O(*m*-$CH_2C_6H_4CH_2$)O-TMP]Rh−I (4e). The iodorhodium(III) diporphyrin complex **4e** was prepared in 74% yield from diporphyrin **3e** by a procedure analogous to that given for complex **4a**. ^{1}H NMR (C_6D_6), δ (ppm): 9.02 (d, 4H, $^3J_{H-H}$ = 4.9 Hz, pyrrole), 8.88 (d, 4H, $^3J_{H-H}$ = 4.9 Hz, pyrrole), 8.83 (s, 8H, pyrrole), 8.14 (dd, 2H, $^3J_{H-H}$ = 8.3 Hz, $^4J_{H-H}$ = 2.2 Hz, *o*-phenyl), 8.00 (dd, 2H, $^3J_{H-H}$ = 8.3 Hz, $^4J_{H-H}$ = 2.2 Hz, o′-phenyl), 7.27 (dd, 2H, $^3J_{H-H}$ = 8.3 Hz, $^4J_{H-H}$ = 2.6 Hz, *m*-phenyl), 7.10 (dd, 2H, $^3J_{H-H}$ = 8.3 Hz, $^4J_{H-H}$ = 2.6 Hz, *m*′-phenyl), 7.24 (s, 6H, *m*″-phenyl), 7.20 (s, 2H, *m*‴-phenyl), 7.10 (s, 2H, *m*⁗-phenyl), 7.08 (s, 6H, *m*⁗⁗-phenyl), 5.00 (s, 4H, $-OCH_{2-}$), 2.45 (s, 18H, *p*-CH_3), 2.33 (s, 12H, *o*-CH_3), 2.22 (s, 6H, *o*′-CH_3), 1.77 (s, 6H, *o*″-CH_3), 1.72 (s, 12H, *o*‴-CH_3). UV−vis ($CHCl_3$), λ_{max} (nm): 532, 420. FAB-MS for $C_{114}H_{98}N_8O_2Rh_2I_2$: *m*/*e* 2071 ($MH^+$), 1925 ($MH^+$ − I), 1798 (MH^+ − 2I). FAB-HRMS (MH^+): calcd for $C_{114}H_{98}N_8O_2Rh_2I_2$, *m*/*e* 2071.4090; found, *m*/*e* 2071.4163.

H_3C−Rh[TMP-O$(CH_2)_6$O-TMP]Rh−CH_3 (5a). The iodorhodium(III) diporphyrin complex **4a** (69.8 mg, 0.034 mmol) was dissolved in ethanol (25 mL) by stirring at 60 °C for 40 min. The resulting deep red solution was filtered in air into a two-neck round-bottom flask and flushed with argon for 40 min. Addition of an excess of $NaBH_4$ (14.2 mg, 0.375 mmol) in aqueous NaOH (0.1 M, 2.0 mL) to the above solution under argon effected a color change from deep red to dark brown, indicating the formation of the Rh^I[TMP-O$(CH_2)_6$O-TMP]Rh^I dianion. The resulting solution was stirred for 1.5 h. Addition of CH_3I (0.2 mL, 3.2 mmol) resulted in the formation of methylrhodium(III) diporphyrin complex **5a** as a light orange precipitate, which was collected by filtration and purified by column chromatography (silica gel, C_6H_6) to give **5a** in 85% yield. The addition of $^{13}CH_3I$ instead of CH_3I afforded the ^{13}C derivative of the complex **5a**, $H_3{}^{13}C$−Rh[TMP-O$(CH_2)_6$O-TMP]Rh−$^{13}CH_3$. ^{1}H NMR (C_6D_6), δ (ppm): 9.00 (d, 4H, $^3J_{H-H}$ = 4.9 Hz, pyrrole), 8.82 (d, 4H, $^3J_{H-H}$ = 4.9 Hz, pyrrole), 8.78 (s, 8H, pyrrole), 8.19 (dd, 2H, $^3J_{H-H}$ = 8.4 Hz, $^4J_{H-H}$ = 2.1 Hz, *o*-phenyl), 8.02 (dd, 2H, $^3J_{H-H}$ = 8.4 Hz, $^4J_{H-H}$ = 2.1 Hz, *o*′-phenyl), 7.31 (dd, 2H, $^3J_{H-H}$ = 8.4 Hz, $^4J_{H-H}$ = 2.6 Hz, *m*-phenyl), 7.18 (dd, 2H, $^3J_{H-H}$ = 8.4 Hz, $^4J_{H-H}$ = 2.6 Hz, *m*′-phenyl), 7.24 (s, 4H, *m*″-phenyl), 7.20 (s, 2H, *m*‴-phenyl), 7.10 (s, 2H, *m*⁗-phenyl), 7.08 (s, 4H, *m*⁗⁗-phenyl), 3.92 (t, 4H, $^3J_{H-H}$ = 6.1 Hz, $-OCH_{2-}$), 2.45 (s, 18H, *p*-CH_3), 2.33 (s, 12H, *o*-CH_3), 2.23 (s, 6H, *o*′-CH_3), 1.78 (s, 6H, *o*″-CH_3), 1.73 (s, 12H, *o*‴-CH_3), 1.86 (m, 4H, $-OCCH_{2-}$), 1.58 (m, 4H, $-CCH_2CH_2C-$), −5.29 (dd, 6H, Rh−$^{13}CH_3$, $^2J_{103Rh-H}$ = 2.9 Hz, $^1J_{13C-H}$ = 141.5 Hz). ^{13}C NMR ($CD_3C_6D_5$), δ (ppm): −13.58 (qd, $^1J_{103Rh-13C}$ = 29 Hz, $^1J_{H-13C}$ = 141.5 Hz). UV−vis (C_6H_6), λ_{max} (nm): 522, 414. FAB-HRMS (M^+): calcd for $C_{112}{}^{13}C_2H_{108}N_8O_2Rh_2$, *m*/*e* 1828.6773; found, *m*/*e* 1828.6842.

H_3C−Rh[TMP-O$(CH_2)_{11}$O-TMP]Rh−CH_3 (5b). The methylrhodium(III) diporphyrin complex **5b** was prepared in 82% yield from the iodorhodium(III) diporphyrin complex **4b** by a procedure analogous to that given for complex **5a**. ^{1}H NMR (C_6D_6), δ (ppm): 8.98 (d, 4H, $^3J_{H-H}$ = 4.9 Hz, pyrrole), 8.81 (d, 4H, $^3J_{H-H}$ = 4.9 Hz, pyrrole), 8.78 (s, 8H, pyrrole), 8.17 (dd, 2H, $^3J_{H-H}$ = 8.4 Hz, $^4J_{H-H}$ = 2.1 Hz, *o*-phenyl), 8.04 (dd, 2H, $^3J_{H-H}$ = 8.4 Hz, $^4J_{H-H}$ = 2.1 Hz, *o*′-phenyl), 7.28 (dd, 2H, $^3J_{H-H}$ = 8.4 Hz, $^4J_{H-H}$ = 2.6 Hz, *m*-phenyl), 7.14 (dd, 2H, $^3J_{H-H}$ = 8.4 Hz, $^4J_{H-H}$ = 2.6 Hz, *m*′-phenyl), 7.24 (s, 4H, *m*″-phenyl), 7.20 (s, 2H, *m*‴-phenyl), 7.08 (s, 4H, *m*⁗⁗-phenyl), 3.92 (t, 4H, $^3J_{H-H}$ = 6.0 Hz, $-OCH_{2-}$), 2.45 (s, 18H, *p*-CH_3), 2.34 (s, 12H, *o*-CH_3), 2.23 (s, 6H, *o*′-CH_3), 1.78 (s, 6H, *o*″-CH_3), 1.73 (s, 12H, *o*‴-CH_3), 1.87 (m, 4H, $-OCCH_{2-}$), 1.58 (m, 4H, $-C(CH_2)_7C-$), −5.29 (dd, 6H, Rh−$^{13}CH_3$, $^2J_{103Rh-H}$ = 2.9 Hz, $^1J_{13C-H}$ = 141.5 Hz). ^{13}C NMR ($CD_3C_6D_5$), δ (ppm): −13.58 (qd, $^1J_{103Rh-13C}$ = 29 Hz, $^1J_{H-13C}$ = 141.5 Hz). UV−vis (C_6H_6), λ_{max} (nm): 523, 413. FAB-HRMS (MH^+): calcd for $C_{117}{}^{13}C_2H_{118}N_8O_2Rh_2$, *m*/*e* 1899.7653; found, *m*/*e* 1899.7697.

H_3C−Rh[DMTMP-O$(CH_2)_5$O-DMTMP]Rh−CH_3 (5c). The methylrhodium(III) diporphyrin complex **5c** was prepared in 84% yield from the iodorhodium(III) diporphyrin complex **4c** by a procedure analogous to that given for complex **5a**. ^{1}H NMR (C_6D_6), δ (ppm): 8.84 (d, 4H, $^3J_{H-H}$ = 4.9 Hz, pyrrole), 8.78 (d, 4H, $^3J_{H-H}$ = 4.9 Hz, pyrrole), 8.76 (s, 8H, pyrrole), 7.22 (s, 8H, arom), 7.08 (s, 4H, arom), 4.01 (t, 4H, $^3J_{H-H}$ = 6.1 Hz, $-OCH_{2-}$), 2.44 (s, 18H, *p*-CH_3), 2.30 (s, 6H, *o*-CH_3), 2.27 (s, 18H, *o*′-CH_3), 1.90 (m, 6H, $-CH_2CH_2CH_{2-}$), 1.78 (s, 6H, *o*″-CH_3), 1.74 (s, 18H, *o*‴-CH_3), −5.24 (d, 6H, $RhCH_3$, $^2J_{Rh-CH_3}$ = 2.8 Hz). ^{13}C NMR ($CD_3C_6D_5$), δ (ppm): −13.58 (qd, $^1J_{103Rh-13C}$ = 29 Hz, $^1J_{H-13C}$ = 141.5 Hz). UV−vis (C_6H_6), λ_{max} (nm): 522, 414. FAB-MS for $C_{117}H_{114}N_8O_2Rh_2$: *m*/*e* 1869 (M^+), 1854 (M^+ − CH_3), 1839 (M^+ − 2CH_3). FAB-HRMS (MH^+): calcd for $C_{117}H_{114}N_8O_2Rh_2$: *m*/*e* 1868.7177; found, *m*/*e* 1868.7102.

H_3C−Rh[DMTMP-O$(CH_2)_6$O-DMTMP]Rh−CH_3 (5d). The methylrhodium(III) diporphyrin complex **5d** was prepared in 80% yield from the iodorhodium(III) diporphyrin complex **4d** by a procedure analogous to that given for complex **5a**. ^{1}H NMR (C_6D_6), δ (ppm): 8.84 (d, 4H, $^3J_{H-H}$ = 4.9 Hz, pyrrole), 8.77 (d, 4H, $^3J_{H-H}$ = 4.9 Hz, pyrrole), 8.76 (s, 8H, pyrrole), 7.21 (s, 8H, *m*-phenyl), 7.07 (s, 8H, *m*′-phenyl), 4.00 (t, 4H, $^3J_{H-H}$ = 5.8 Hz, $-OCH_{2-}$), 2.44 (s, 18H, *p*-CH_3), 2.29 (s, 6H, *o*′-CH_3), 2.27 (s, 18H, *o*″-CH_3), 1.78 (s, 6H, *o*‴-CH_3), 1.74 (s, 18H, *o*⁗-CH_3), 1.85 (m, 4H, $-OCCH_{2-}$), 1.66 (m, 4H, $-CCH_2CH_2C-$), −5.25 (dd, 6H, Rh−$^{13}CH_3$, $^2J_{103Rh-H}$ = 2.9 Hz, $^1J_{13C-H}$ = 141.5 Hz). ^{13}C NMR (C_6D_6), δ (ppm): −14.00 (qd, $^1J_{103Rh-13C}$ = 29 Hz, $^1J_{H-13C}$ = 141.5 Hz). UV−vis (C_6H_6), λ_{max} (nm): 522, 415. FAB-HRMS (M^+): calcd for $C_{118}H_{116}N_8O_2Rh_2$, *m*/*e* 1882.7333; found, *m*/*e* 1882.7403.

H_3C−Rh[TMP-O(*m*-$CH_2C_6H_4CH_2$)O-TMP]Rh−CH_3 (5e). The

methylrhodium(III) diporphyrin complex **5e** was prepared in 85% yield from the iodorhodium(III) diporphyrin complex **4e** by a procedure analogous to that given for complex **5a**. ^{1}H NMR (C_6D_6), δ (ppm): 8.97 (d, 4H, $^3J_{H-H}$ = 4.9 Hz, pyrrole), 8.81 (d, 4H, $^3J_{H-H}$ = 4.9 Hz, pyrrole), 8.77 (s, 8H, pyrrole), 8.16 (dd, 2H, $^3J_{H-H}$ = 8.3 Hz, $^4J_{H-H}$ = 2.2 Hz, *o*-phenyl), 8.03 (dd, 2H, $^3J_{H-H}$ = 8.3 Hz, $^4J_{H-H}$ = 2.2 Hz, *o*′-phenyl), 7.33 (dd, 2H, $^3J_{H-H}$ = 8.3 Hz, $^4J_{H-H}$ = 2.6 Hz, *m*-phenyl), 7.17 (dd, 2H, $^3J_{H-H}$ = 8.3 Hz, $^4J_{H-H}$ = 2.6 Hz, *m*′-phenyl), 7.24 (s, 6H, *m*″-phenyl), 7.20 (s, 2H, *m*‴-phenyl), 7.10 (s, 2H, *m*⁗-phenyl), 7.08 (s, 6H, *m*⁗′-phenyl), 5.00 (s, 4H, $-OCH_{2-}$), 2.45 (s, 18H, *p*-CH_3), 2.33 (s, 12H, *o*-CH_3), 2.22 (s, 6H, *o*′-CH_3), 1.77 (s, 6H, *o*″-CH_3), 1.72 (s, 12H, *o*‴-CH_3), −5.31 (dd, 6H, Rh−$^{13}CH_3$, $^2J_{103Rh-H}$ = 2.9 Hz, $^1J_{13C-H}$ = 141.5 Hz). ^{13}C NMR ($CD_3C_6D_5$), δ (ppm): −13.6 (qd, $^1J_{103Rh-13C}$ = 29 Hz, $^1J_{H-13C}$ = 141.5 Hz). FAB-HRMS (MH^+): calcd for $C_{114}{}^{13}C_2H_{104}N_8O_2Rh_2$, *m*/*e* 1849.6537; found, *m*/*e* 1849.6530.

[·Rh^{II}[TMP-O(CH$_2$)$_6$O-TMP]Rh^{II}·] (6a). Degassed benzene solution of the methylrhodium(III) diporphyrin complex **5a** (0.5−0.8 mg/0.3 mL) in a vacuum-adapted NMR tube was photolyzed (λ > 350 nm) for 6 h in a Rayonet photoreactor. The solvent along with methane and toluene formed in the reaction were removed under vacuum to give **6a** as a solid in quantitative yield. ^{1}H NMR (C_6D_6, 296 K), δ (ppm): 18.57 (br s, 16H, pyrrole), 11.36 (br s, 8H, *o*-H + *m*-H), 8.90 (s, 12H, *m*′-H), 5.10 (s, 4H, $-OCH_{2-}$), 3.58 (br s, 36H, *o*-CH_3), 3.52 (s, 18H, *p*-CH_3), 2.77 (s, 8H, $-CH_2CH_2CH_2CH_{2-}$). A linear relationship between the pyrrole chemical shift vs the inverse temperature was obtained from the temperature dependence study. EPR (90 K, toluene): $g_{1,2}$ = 2.64, g_3 = 1.90, $A(^{103}Rh)g_3 \sim$ 158 MHz. EPR for the triphenylphosphine adduct **7a** (90 K, toluene): $g_{1,2}$ = 2.17, g_3 = 2.00, $A(^{31}P)g_{1,2}$ = 756 MHz, $A(^{31}P)g_3$ = 1016 MHz, $A(^{103}Rh)g_3$ = 61 MHz. EPR for the superoxo complex of the triphenylphosphine adduct **8a** (90 K, toluene): g_1 = 2.08, g_2 = 2.005, g_3 = 1.996, $A(^{31}P)g_1$ = 50.9 MHz, $A(^{31}P)g_2$ = 50.5 MHz, $A(^{31}P)g_3$ = 50.3 MHz.

[·Rh(II)[TMP-O(CH$_2$)$_{11}$O-TMP]Rh(II)·] (6b). The rhodium(II) porphyrin bimetalloradical complex **6b** was prepared in quantitative yield from the methylrhodium(III) diporphyrin complex **5b** by a procedure analogous to that given for bimetalloradical **6a**. ^{1}H NMR (C_6D_6, 296 K), δ (ppm): 18.57 (br s, 16H, pyrrole), 11.36 (br s, 8H, *o*-H + *m*-H), 8.90 (s, 12H, *m*′-H), 5.10 (s, 4H, $-OCH_{2-}$), 3.58 (br s, 36H, *o*-CH_3), 3.52 (s, 18H, *p*-CH_3), 2.77 (s, 18H, $-(CH_2)_{9-}$). A linear relationship between the pyrrole chemical shift vs the inverse temperature was obtained from the temperature dependence study. EPR (90 K, toluene): $g_{1,2}$ = 2.64, g_3 = 1.90, $A(^{103}Rh)g_z \sim$ 158 MHz.

[·Rh(II)[DMTMP-O(CH$_2$)$_5$O-DMTMP]Rh(II)·] (6c). The rhodium(II) porphyrin bimetalloradical complex **6c** was prepared in quantitative yield from the methylrhodium(III) diporphyrin complex **5c** by a procedure analogous to that given for bimetalloradical **6a**. ^{1}H NMR (C_6D_6), δ (ppm): 18.45 (broad, 16H, pyrrole H), 8.88 (broad, 16H, arom), 3.57 (br s, 48H, *o*-CH_3), 3.51 (s, 18H, *p*-CH_3). A linear relationship between the pyrrole chemical shift vs the inverse temperature was obtained from the temperature dependence study. UV−vis (C_6H_6), λ_{max} (nm): 538, 426. FAB-MS for $C_{115}H_{107}N_8O_2Rh_2$: *m*/*e* 1840 (MH^+).

[·Rh(II)[DMTMP-O(CH$_2$)$_6$O-DMTMP]Rh(II)·] (6d). The rhodium(II) porphyrin bimetalloradical complex **6d** was prepared in quantitative yield from the methylrhodium(III) diporphyrin complex **5d** by a procedure analogous to that given for bimetalloradical **6a**. ^{1}H NMR (C_6D_6, 296 K), δ (ppm): 18.50 (br s, 16H, pyrrole), 8.87 (s, 16H, *m*-phenyl), 5.22 (s, 4H, $-OCH_{2-}$), 3.57 (br s, 48H, *o*-CH_3), 3.51 (s, 18H, *p*-CH_3), 2.90 (s, 8H, $-CH_2CH_2CH_2CH_{2-}$). A linear relationship between the pyrrole chemical shift vs the inverse temperature was obtained from the temperature dependence study. UV−vis (C_6H_6), λ_{max} (nm): 538, 426. FAB-MS for $C_{116}H_{110}N_8O_2Rh_2$: *m*/*e* 1854 (MH^+).

[·Rh(II)[TMP-O(*m*-CH$_2$C$_6$H$_4$CH$_2$)O-TMP]Rh(II)·] (6e). The rhodium(II) porphyrin bimetalloradical complex **6e** was prepared in quantitative yield from the methylrhodium(III) diporphyrin complex **5e** by a procedure analogous to that given for bimetalloradical **6a**. ^{1}H NMR (C_6D_6), δ (ppm): 18.4 (br s, 16H, pyrrole), 11.3 (br s, 8H, *o*-H + *m*-H), 8.90 (s, 16H, *m*′-H), 5.10 (s, 4H, $-OCH_{2-}$), 3.58 (br s, 36H, *o*-CH_3), 3.51 (s, 18H, *p*-CH_3). A linear relationship between the pyrrole chemical shift vs the inverse temperature was obtained from the temperature dependence study. EPR (90 K, toluene): $g_{1,2}$ = 2.64, g_3 = 1.90, $A(^{103}Rh)g_3 \sim$ 158 MHz.

Reactions of **6a**−**e** with Hydrogen. Weighed samples of CH_3–(TMP-O(CH$_2$)$_n$O-TMP)Rh−CH_3 (**5**) (∼0.5 mg) were placed in vacuum-adapted NMR tubes and evacuated prior to vacuum transfer of C_6D_6 (∼0.5 mL) as solvent. The solutions were photolyzed for 6 h in a Rayonet photoreactor (λ > 350 nm) which is known to result in the complete conversion of CH_3–(TMP-O(CH$_2$)$_n$O-TMP)Rh−CH_3 (**5**) to ·Rh(TMP-O(CH$_2$)$_n$O-TMP)Rh· (**6**). The benzene-d_6 solution of ·Rh-(TMP-O(CH$_2$)$_n$O-TMP)Rh· (**6**) was evacuated to dryness followed by sequential vacuum transfer of C_6D_6 (∼0.6 mL) and hydrogen gas (P = 540 Torr). The products were identified as H−(TMP-O(CH$_2$)$_n$O-TMP)Rh−H (**8**).

(1) H−Rh[TMP-O(CH$_2$)$_6$O-TMP]Rh−H (7a): ^{1}H NMR (C_6D_6) δ 8.96 (d, 2H, $^3J_{H-H}$ = 4.9 Hz, pyrrole), 8.81 (d, 2H, $^3J_{H-H}$ = 4.9 Hz, pyrrole), 8.80 (d, 2H, $^3J_{H-H}$ = 4.9 Hz, pyrrole), 8.79 (d, 2H, $^3J_{H-H}$ = 4.9 Hz, pyrrole), 8.15 (dd, 1H, $^3J_{H-H}$ = 8.4 Hz, $^4J_{H-H}$ = 2.1 Hz, *o*-phenyl), 7.92 (dd, 1H, $^3J_{H-H}$ = 8.4 Hz, $^4J_{H-H}$ = 2.1 Hz, *o*′-phenyl), 7.28 (dd, 1H, $^3J_{H-H}$ = 8.4 Hz, $^4J_{H-H}$ = 2.6 Hz, *m*′-phenyl), 7.10 (dd, 1H, $^3J_{H-H}$ = 8.4 Hz, $^4J_{H-H}$ = 2.6 Hz, *m*′-phenyl), 7.23 (s, 4H, *m*″-phenyl), 7.19 (s, 2H, *m*‴-phenyl), 7.11 (s, 6H, *m*⁗-phenyl), 3.92 (t, 4H, $^3J_{H-H}$ = 6.1 Hz, $-OCH_{2-}$), 2.45 (s, 12H, *p*-CH_3), 2.43 (s, 6H, *p*′-CH_3), 2.28 (s, 12H, *o*′-CH_3), 2.05 (s, 6H, *o*′-CH_3), 1.87 (s, 6H, *o*″-CH_3), 1.76 (s, 12H, *o*⁗-CH_3), 1.86 (m, 4H, $-OCCH_{2-}$), 1.57 (m, 4H, $-CCH_2CH_2C-$), −40.07 (d, 1H, Rh−H, $^1J_{103Rh-H}$ = 43.4 Hz,); FAB MS for $C_{112}H_{104}H_8O_2Rh_2$, *m*/*e* 1798 ($M^{+\ -}$ H).

(2) H−Rh[TMP-O(CH$_2$)$_{11}$O-TMP]Rh−H (**7b**): ^{1}H NMR (C_6D_6) δ 8.94 (d, 2H, $^3J_{H-H}$ = 4.9 Hz, pyrrole), 8.81 (d, 2H, $^3J_{H-H}$ = 4.9 Hz, pyrrole), 8.80 (d, 2H, $^3J_{H-H}$ = 4.9 Hz, pyrrole), 8.79 (d, 2H, $^3J_{H-H}$ = 4.9 Hz, pyrrole), 8.12 (dd, 1H, $^3J_{H-H}$ = 8.4 Hz, $^4J_{H-H}$ = 2.1 Hz, *o*-phenyl), 7.88 (dd, 1H, $^3J_{H-H}$ = 8.4 Hz, $^4J_{H-H}$ = 2.1 Hz, *o*′-phenyl), 7.26 (dd, 1H, $^3J_{H-H}$ = 8.4 Hz, $^4J_{H-H}$ = 2.6 Hz, *m*-phenyl), 7.06 (dd, 1H, $^3J_{H-H}$ = 8.4 Hz, $^4J_{H-H}$ = 2.6 Hz, *m*′-phenyl), 7.23 (s, 6H, *m*″-phenyl), 7.11 (s, 6H, *m*‴-phenyl), 7.11 (s, 6H, *m*⁗-phenyl), 3.92 (t, 4H, $^3J_{H-H}$ = 6.1 Hz, $-OCH_{2-}$), 2.45 (s, 12H, *p*-CH_3), 2.43 (s, 6H, *p*′-CH_3), 2.28 (s, 12H, *o*′-CH_3), 2.05 (s, 6H, *o*′-CH_3), 1.87 (s, 6H, *o*″-CH_3), 1.75 (s, 12H, *o*‴-CH_3), 1.87 (m, 4H, $-OCCH_{2-}$), 1.58 (m, 4H, $-C(CH_2)_7C-$), −40.07 (d, 1H, Rh−H, $^1J_{103Rh-H}$ = 43.5 Hz).

(3) H−Rh[DMTP-O(CH$_2$)$_5$O-DMTMP]Rh−H (**7c**): ^{1}H NMR (C_6D_6) δ 8.86−8.75 (m, 16H, pyrrole H), 7.22, 7.08 (two s, 16H, arom), 4.01 (t, 4H, $-CH_2O$), 2.44 (s, 18H, *p*-CH_3), 2.29−2.15 (five s, 24H, *o*-CH_3), 1.90 (m, 6H, $-CH_2CH_2CH_{2-}$), 1.84, 1.80 (two s, 24H, *o*-CH_3), −40.00 (d, 1H, Rh−H, $J_{Rh-H'}$ = 43.4 Hz).

(4) H−Rh[DMTMP-O(CH$_2$)$_6$O-DMTMP]Rh−H (**7d**): ^{1}H NMR (C_6D_6) δ 8.85−8.75 (m, 16H, pyrrole H), 7.22 (s, 8H, *m*-phenyl), 7.08 (s, 8H, *m*-phenyl), 4.00 (t, 4H, $-CH_2O$), 2.43 (s, 18H, *o*′-CH_3), 2.29 (s, 6H, *o*′-CH_3), 2.27 (s, 18H, *o*″-CH_3), 1.80 (s, 6H, *o*‴-CH_3), 1.74 (s, 18H, *o*⁗-CH_3), 1.85 (m, 4H, $-OCCH_{2-}$), 1.66 (m, 4H, $-CCH_2CH_2C-$), −40.00 (d, 1H, Rh−H, $J_{Rh-H'}$ = 43.4 Hz).

(5) H−Rh[TMP-O(*m*-CH$_2$C$_6$H$_4$CH$_2$)O-TMP]Rh−H (**7e**): ^{1}H NMR (C_6D_6) δ 8.93 (d, 4H, $^3J_{H-H}$ = 4.9 Hz, pyrrole), 8.81 (d,4H, $^3J_{H-H}$ = 4.9 Hz, pyrrole), 8.80 (d, 4H, $^3J_{H-H}$ = 4.9 Hz, pyrrole), 8.79 (d, 4H, $^3J_{H-H}$ = 4.9 Hz, pyrrole), 8.12 (dd, 2H, $^3J_{H-H}$ = 8.4 Hz, $^4J_{H-H}$ = 2.2 Hz, *o*-phenyl), 7.89 (dd, 2H, $^3J_{H-H}$ = 8.3 Hz, $^4J_{H-H}$ = 2.2 Hz, *o*′-phenyl), 7.30 (dd, 2H, $^3J_{H-H}$ = 8.3 Hz, $^4J_{H-H}$ = 2.6 Hz, *m*-phenyl), 7.15 (dd, 2H, $^3J_{H-H}$ = 8.3 Hz, $^3J_{H-H}$ = 2.6 Hz, *m*′-phenyl), 7.75 (s, 1H, spacer-phenyl), 7.43 (d, 2H, $^3J_{H-H}$ = 7.4 Hz, spacer-phenyl), 7.35 (t, 1H, $^3J_{H-H}$ = 7.4 Hz, spacer-phenyl), 7.22 (s, 4H, *m*″-phenyl), 7.20 (s, 2H, *m*‴-phenyl), 7.11 (s, 2H, *m*⁗-phenyl), 7.10 (s, 4H, *m*⁗′-phenyl), 5.00 (s, 4H, $-OCH_{2-}$), 2.44 (s, 12H, *p*-CH_3), 2.43 (s, 6H, *p*′-CH_3), 2.28 (s, 12H, *o*-CH_3), 2.04 (s, 6H, *o*′-CH_3), 1.87 (s, 6H, *o*″-CH_3), 1.75 (s, 12H, *o*‴-CH_3), −40.09 (d, 1H, Rh−H, J_{Rh-H} = 43.5 Hz).

Acknowledgment. This research was supported by the Department of Energy Division of Chemical Sciences, Office of Science, through Grant DE-FG02-86ER-13615. <<

IC0006302